

Autophagy is dispensable for B-cell development but essential for humoral autoimmune responses

J Arnold¹, D Murera¹, F Arbogast¹, J-D Fauny¹, S Muller^{1,2} and F Gros^{*,1,3}

To gain new insight into the role of B-cell autophagy, we generated two novel mouse models deficient for the autophagy-related gene (*Atg5*), one from the outset pro-B cell stage (*Atg5*^{fl/fl} Mb1 cre) and the other in mature B cells only (*Atg5*^{fl/fl} CD21 cre). We show that autophagy is dispensable for pro- to pre-B cell transition, but necessary at a basal level to maintain normal numbers of peripheral B cells. It appears non-essential for B-cell activation under B-cell receptor stimulation but required for their survival after lipopolysaccharide stimulation that drives plasmablast differentiation and for specific IgM production after immunization. Results obtained using *Atg5*^{fl/fl} CD21 cre × C57BL/6^{lpr/lpr} autoimmune-prone mice show that B-cell autophagy is involved in the maintenance of anti-nuclear antibody secretion, elevated number of long-lived plasma cells, and sustains IgG deposits in the kidneys. Thus, treatments specifically targeting autophagy might be beneficial in systemic autoimmune diseases.

Cell Death and Differentiation (2016) 23, 853–864; doi:10.1038/cdd.2015.149; published online 20 November 2015

Macroautophagy is a catabolic process allowing the degradation of cytoplasmic material in double membrane vesicles, ultimately fusing with lysosomes. Macroautophagy, initially implicated in the generation of nutrients under metabolic stress, is known to have multiple roles, in different physiologic compartments, such as in vacuole trafficking, cell signalling, and cell death. Macroautophagy is deeply involved in the regulation of immunity.¹ It has been shown that autophagy can regulate inflammation related to inflammasome activation and to type I interferon secretion. Moreover, it contributes to antigen presentation by both major histocompatibility complex (MHC) class I and class II molecules.²

Macroautophagy is also tightly linked to lymphocyte activation and survival. It has central roles in T-cell basal homeostasis, survival, and polarization.³ It is also involved in the regulation of T-cell signalling by downregulating the NF- κ B pathway⁴ and apoptosis processes through the procaspases 3 and 8 degradation.⁵

Macroautophagy has additionally been described to regulate B-cell lineage, in particular during B-cell development. Thus, it has been shown that B cells generated from fetal liver chimaeras, with a complete deletion of the essential autophagy-related gene (*Atg5*), exhibited a block at the pro- to pre-B stage transition.^{6,7} However, as the genetic deletion is systemic and occurs very early during development, the question remains over whether the developmental blockade could be due to defects resulting from early haematopoietic development. Indeed, macroautophagy has been shown to be fundamental to haematopoietic stem cell survival and

renewal.⁸ Moreover, conditional deletion of *Atg5* under the control of CD19 promoter expressed from the pre-B stage does not lead to major developmental breaks, except a decrease in B-1a B-cell population.⁶ The contrast with results obtained with chimaeric mice could be due to the partial deletion induced by cre expression under the control of CD19 promoter.⁹ At this stage, however, it remains unclear whether macroautophagy is really needed in the first steps of B-cell development.

Studies based on mouse models deleted for autophagy genes at an early stage of development led to fundamental findings regarding the importance of macroautophagy in B cell-related immune responses. Two independent studies, based on T cell-dependent and -independent model antigens or on infectious agents,^{10,11} concluded that macroautophagy is necessary *in vivo* for humoral immune responses by regulating plasma cell differentiation and survival. The former study¹¹ showed that macroautophagy is involved in regulating endoplasmic reticulum (ER) load along with plasma cell differentiation, thus limiting ER stress and contributes to long-lived plasma cell survival. A role for macroautophagy in B-cell early activation was excluded, especially in germinal centre (GC) formation. Two more recent studies, one based on a mouse model of influenza infection and the other on model antigens used as immunogens, demonstrated that in addition to its effect on plasma cell survival, macroautophagy is necessary for the survival of B-cell memory compartment.^{12,13} These findings therefore also implicate macroautophagy in humoral autoimmunity.

¹CNRS, Immunopathology and Therapeutic Chemistry/Laboratory of Excellence MEDALIS, Institut de Biologie Moléculaire et Cellulaire, Strasbourg, France; ²University of Strasbourg Institute for Advanced Study, Strasbourg, France and ³University of Strasbourg, Strasbourg, France

*Corresponding author: F Gros, IBMC UPR3572, CNRS/Université de Strasbourg, 15 rue Descartes, Strasbourg 67084, France. Tel: +33(3) 88417024; Fax: +33(3) 88610680; E-mail: f.gros@ibmc-cnrs.unistra.fr

Abbreviations: Abs, antibodies; ACTB, β -actin; *Atg*, autophagy-related genes; BCR, B-cell receptor; CFA/IFA, complete/incomplete Freund adjuvant; CFSE, carboxyfluorescein succinimidyl ester; CMA, chaperone-mediated autophagy; dsDNA, double-stranded DNA; ER, endoplasmic reticulum; FO, follicular; GC, germinal centre; IRF4, interferon-responding factor 4; LC3, light-chain 3 standing for *MAP1LC3B*, microtubule-associated protein light-chain 3B; LPS, lipopolysaccharide; MHC, major histocompatibility complex; MZ, marginal zone; OVA, ovalbumin; PNA, peanut agglutinin; SLE, systemic lupus erythematosus; T1 and T2, transitional 1 and 2; TCR, T-cell receptor

Received 24.4.15; revised 04.10.15; accepted 12.10.15; Edited by M Piacentini; published online 20.11.15

Studying the involvement of autophagy in autoimmunity is justified by its central regulatory impact in inflammation and its role on antigen presentation and on lymphocyte activation and survival.^{14,15} Our team and others described a deregulation of macroautophagy in T cells from both lupus-prone mice and patients suffering from systemic lupus erythematosus (SLE).^{16–18} This deregulation could contribute to autoreactive T-cell survival and can be put in line with the deregulation of both macroautophagy and chaperone-mediated autophagy (CMA) in B cells that has been recently described to occur in lupus.^{19,20} To date, however, these data remain correlative and no study has been published describing an *in vivo* model, prone to systemic autoimmunity, with specific autophagy deletion in B cells.

Here, we describe the generation of two new mouse models of conditional ATG5 deletion, one under the control of a promoter active early during B-cell development (Mb1 cre) and the other active in mature B cells only (CD21 cre). They were designed and constructed to clarify the role of macroautophagy in B-cell development and homeostasis. Comparison of the two models should allow us to define whether identified defects are linked to developmental issues or deregulation of homeostasis. In addition, *Atg5*^{-/-} CD21 cre autophagy-deficient mice were crossed with autoimmune-prone animals to further examine the role of macroautophagy *in vivo* on long-term humoral autoimmunity and study some lupus-related pathophysiological features.

Results

Basal levels of autophagy are necessary for B-cell maintenance. We generated two new mouse models deficient for ATG5 specifically in B cells. The first one, with cre recombinase expression under the control of Mb1 promoter, was deleted early during B-cell development while the second one, under the control of CD21 promoter, was designed to be deleted in mature B cells only. Both mouse models were born at the predicted Mendelian ratio and showed no particular morphologic phenotype.

Atg5^{-/-} CD21 cre (CD21 cre) mice exhibited no deletion of ATG5 in splenic T cells and in these cells, conversion of LC3-I to LC3-II occurred normally (Figure 1a). However, as expected, B cells from CD21 cre mice showed a specific deletion of ATG5 compared with B6 mice (wild type, WT) and littermate *Atg5*^{+/+} CD21 cre mice at both transcriptional and protein levels (Figures 1b and d). A poor conversion of LC3 was observed in *Atg5*^{-/-} CD21 cre mice validating the impeding of the autophagy process, even under stimulation by anti-IgM. As previously reported by others,¹⁹ no increase in autophagic activity was found after BCR stimulation in WT and littermate mice. We also checked whether autophagy was decreased in B cells from *Atg5*^{-/-} Mb1 cre (Mb1 cre) mice. We saw a very efficient deletion of ATG5 in splenic B cells from *Atg5*^{-/-} Mb1 cre mice, correlating with a total impairment of LC3-II generation (Figures 1c and d). *Atg5* mRNA expression was reproducibly lower than for CD21 cre B cells. Although B cells from CD21 cre mice exhibited a reproducible LC3-II knockdown (Figure 1d), LC3-II was no longer observed in Mb1 cre B cells, arguing for a specific deletion of autophagy that is

stronger in this model than in CD21 cre mice. Although ATG5 deletion is observed in littermates relative to both CD21 cre and Mb1 cre mice compared with WT C57BL/6 mice, autophagy levels (deduced from LC3-II staining) were comparable and no significant difference was observed in terms of autophagic flux intensity (Supplementary Figure S1).

To more specifically evaluate the potential autophagy-independent effects of decreased ATG5 expression on phenotypes of both littermates, we then conducted a series of experiments using CD21 cre and Mb1 cre mice separately compared with WT mice. First, we quantified the different subpopulations of B cells in the spleen of these two defective models. Although both types of littermate mice exhibited levels of B cells comparable to wild-type mice, both Mb1 cre and CD21 cre mice showed a diminished number of B cells in the spleen (Figures 2a and b). A decrease in follicular B-cell number and T1 B cells was also observed in both CD21 cre and Mb1 cre mice, as compared with WT mice. However, the homeostatic defect of follicular (FO) B cells in CD21 cre was less severe than in Mb1 cre mice, arguing for a more efficient autophagy impairment in the latter deletion strategy, as described above in Figure 1. Mb1 cre T2 B cells were also diminished compared with the corresponding littermates. However, marginal zone B cells were not seen to be affected by autophagy deletion in both deletion models. These results led us to propose that *Atg5* deletion in B cells induces a defect in peripheral homeostasis, the latter being more pronounced in the context of Mb1 cre-mediated deletion.

Next, we assessed the repartition of B-cell populations from the peritoneum. A decrease in both B-1a and B-2 B-cell proportions was observed in Mb1 cre mice while, in contrast, a decrease in peritoneal B-2 B cells only was visualized in CD21 cre mice (Figures 2f and g). This finding led us to conclude that early during development, autophagy is necessary for the generation of B-1a B cells. The loss of B-2 cells in both mice might be due to sensitivity to cell death of these Ab-secreting cells in the absence of autophagy, or to a defective replenishment from circulating cells.

Altogether, these results show that autophagy is central during development for B-1a B-cell generation. Basal levels of autophagy are necessary to maintain a normal number of B cells in the periphery. B-2 B cells of the peritoneum are particularly sensitive to the decrease in autophagic activity.

Basal levels of autophagy are not necessary for B-2 B-cell development.

The survival defects of peripheral B cells found in Mb1 cre mice could be linked to a developmental issue as described in earlier studies using bone marrow fetal liver chimaeras.⁶ This does not seem to be only attributable to developmental issues as some defects were also found in CD21 cre mice. We checked the number of precursor cells of the B-cell lineage in the bone marrow of Mb1 cre and CD21 cre mice, and compared the data with WT and littermate mice (Figures 3a and b). As expected, no anomaly in B-cell number or in subset distribution was detected in CD21 cre mice when autophagy deletion occurs later during development (Figures 3c and f). In sharp contrast with previous studies,⁶ we did not find any significant decrease in the number of B-cell precursors in Mb1 cre mice. Previous data suggested a developmental block at the

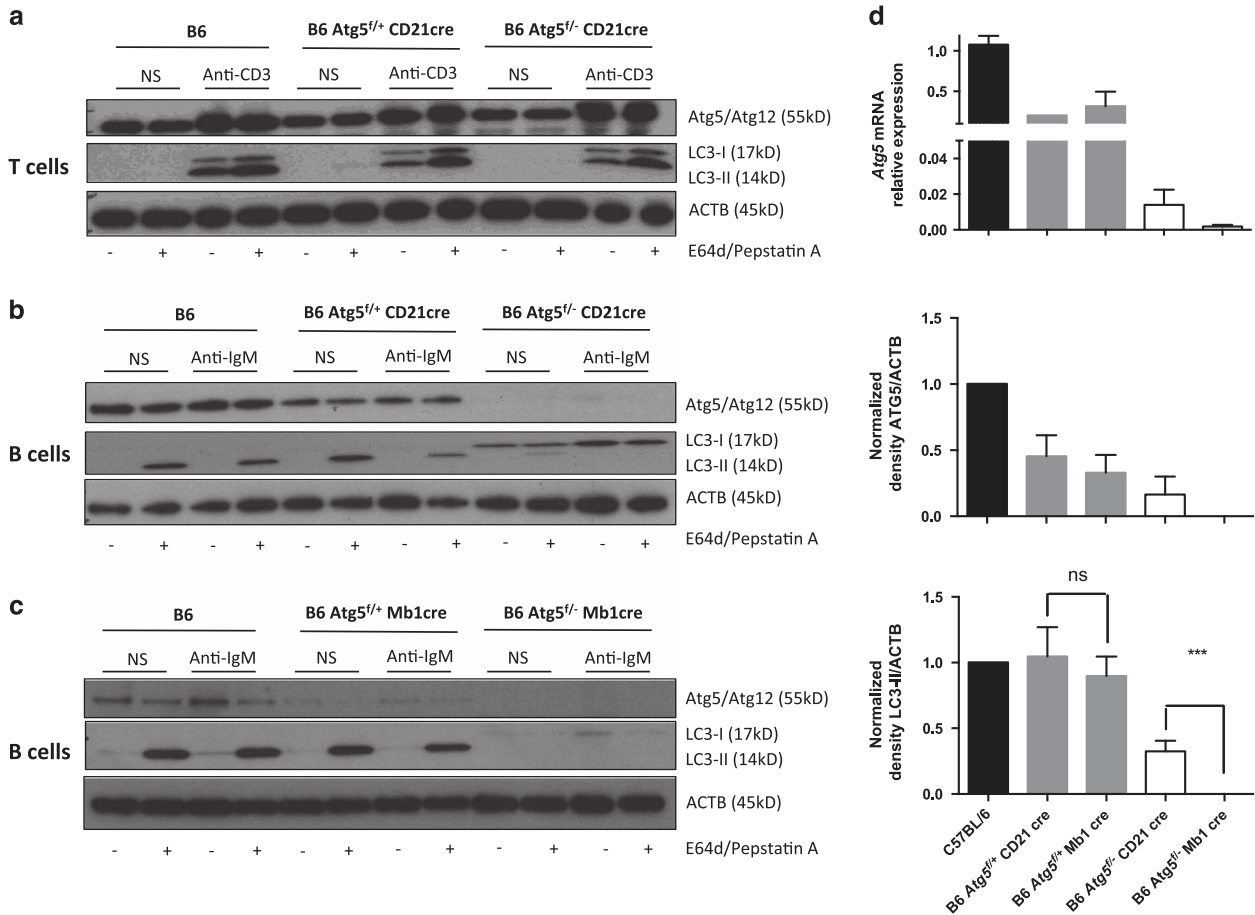


Figure 1 Efficient invalidation of autophagy in B cells from *Atg5^{-/-}* CD21 cre mice and *Atg5^{-/-}* Mb1 cre mice. *Atg5^{+/+}* CD21 cre, *Atg5^{-/-}* CD21 cre, *Atg5^{-/-}* Mb1 cre, and *Atg5^{+/+}* Mb1 cre were generated. B or T cells were purified from the spleen and cultured *in vitro* in the presence of different stimuli. Lysosomal protease inhibitors pepstatin A and E64d were added (+) or not (-) in the indicated conditions. (a) T cells from wild-type C57BL/6 mice (B6), *Atg5^{+/+}* CD21 cre, or *Atg5^{-/-}* CD21 cre were left unstimulated (non-stim) or stimulated by anti-CD3 Ab for 18 h. Cells were lysed and immunoblots were performed against ATG5, LC3, and ACTB. (b and c) B cells from wild-type B6, *Atg5^{+/+}* CD21 cre or *Atg5^{-/-}* CD21 cre (b), *Atg5^{-/-}* Mb1 cre or *Atg5^{+/+}* Mb1 cre (c) were left unstimulated (non-stim) or stimulated by anti-IgM Ab for 18 h. Cells were lysed and immunoblots were performed against ATG5, LC3, and ACTB. (d) Upper panel. Quantification of *Atg5* transcripts in B cells by real-time PCR relative to *Gapdh* expression. One sample from B6 mouse was used for each plate for normalization and its value is arbitrarily set to 1. Middle and lower panels. Densitometric analysis of ATG5 and LC3-II expressions relative to ACTB. The values corresponding to the non-stimulated condition in the presence of protease inhibitors were collected, and normalized to the ratios obtained from B6 wild-type mice on each blot to normalize results. The histograms represent the means with S.E.M. obtained for at least three and seven different blots, respectively, for ATG5 and LC3-II quantification. ns, non-significant; *** $P < 0.001$ (Mann-Whitney *U*-test)

transition between the pro- and pre-B cell stages.⁶ In this study, normal proportions of pro- and immature B cells were detected in the bone marrow of early ATG5-deleted mice (Figures 3c and d). Distinction of pre-B and immature B cells from pro-B cells by CD43 staining did not reveal any decrease in the proportion of pre-B cells in Mb1 cre mice, but instead showed an increase in this population (Figures 3e and f). Thus, autophagy seems dispensable for the pro- to pre-B cell differentiation. However, as previously described by others⁶ using CD19 cre mice, we observed a decrease in the proportion of mature B cells, corresponding to Fraction F defined from Hardy nomenclature (Figures 3c and f).²¹ As the overall number of B cells does not vary between Mb1 cre and their littermates, the increased proportion of pre-B cells in these mice could reflect a spatial compensation consecutive to the loss of mature B cells. As these latter cells are described as recirculating cells coming from the periphery,

they may not necessarily constitute a final developmental stage occurring in the bone marrow. They have also been considered as cells secreting Abs against blood-borne pathogens.²² The acute deletion of autophagy in Mb1 cre mice might thus lead to sensitivity to cell death of this B-cell subtype, because of their long-lived nature or of their Ab secretion properties.

Taken together, these results show that autophagy is dispensable for the transition between pro- and pre-B cell stage. However, basal levels of autophagy are necessary to maintain a normal number of mature recirculating B cells in the bone marrow.

Autophagy is dispensable for B-cell activation in response to BCR stimulation. We then assessed in our two models the potential relevance of autophagy activation in B-cell response to BCR stimulation. We found no difference

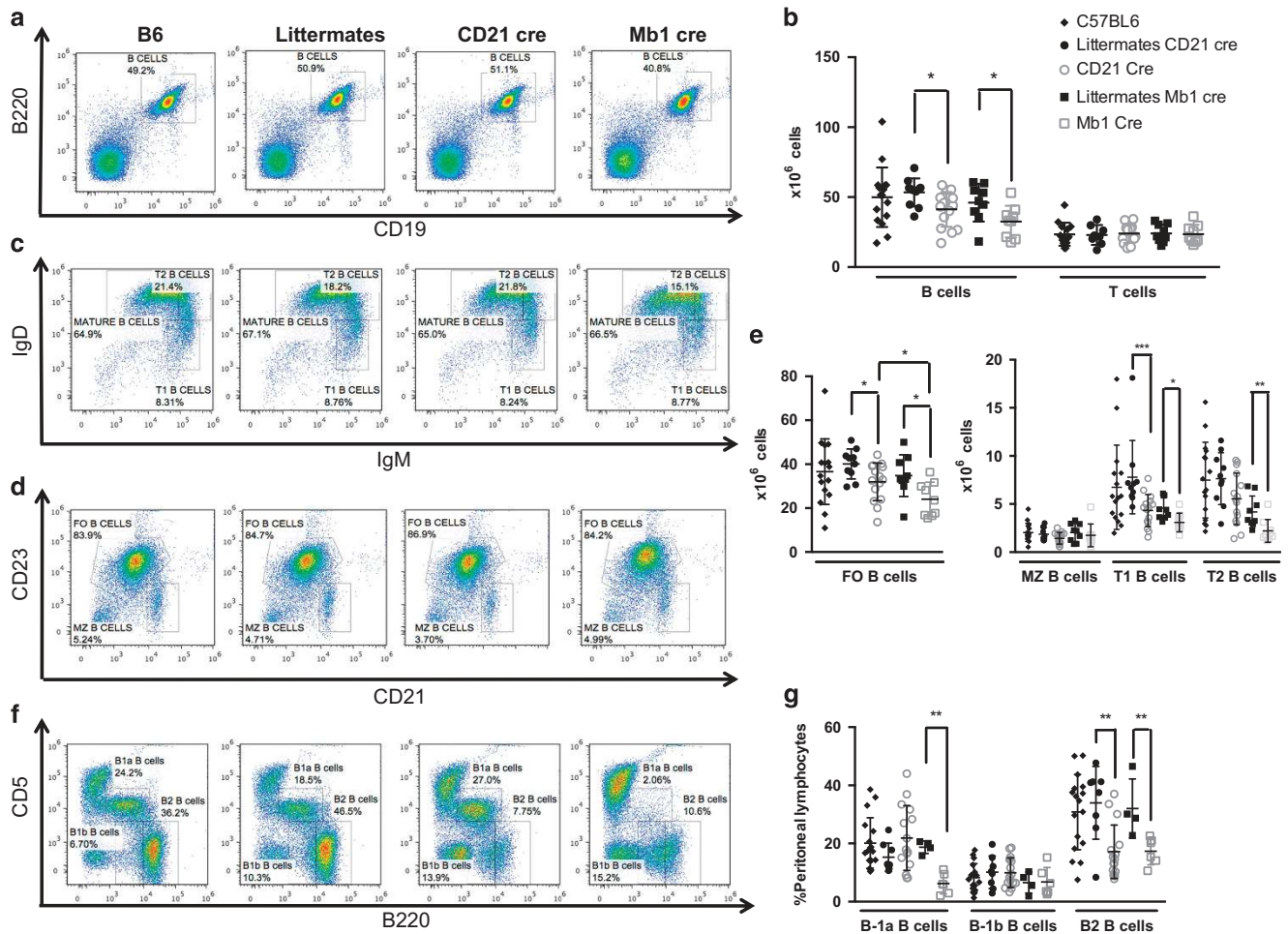


Figure 2 Basal levels of autophagy are necessary for B-cell survival in the periphery. Spleen cells from wild-type C57BL/6 mice (B6), $Atg5^{+/+}$ CD21 cre (littermates CD21 cre) or $Atg5^{+/+}$ Mb1 cre (littermates Mb1 cre), $Atg5^{fl/fl}$ CD21 cre (CD21 cre) or $Atg5^{fl/fl}$ CD21 cre (Mb1 cre) were stained with anti-B220 and anti-CD19 Abs. (a and b) Representative dot plots obtained after flow-cytometry analysis are depicted in (a) showing the percentages of B220⁺CD19⁺ B cells. (b) Individual values for each mouse tested of absolute numbers of B and T cells, in the spleen obtained from B6 mice $n = 16$, littermate CD21 cre mice $n = 10$, littermate Mb1 cre mice $n = 9$, CD21 cre mice $n = 15$, and Mb1 cre mice $n = 9$. Means and standard deviations (S.D.) are indicated. (c–e) Expression was assessed for the spleen of the same animals for the expression of (c) IgD, IgM and (d) CD21 and CD23. Representative dot plots after flow-cytometry analysis show the percentages among B220⁺ cells of mature B cells (IgM^{low}IgD^{hi}), transitional 1 and 2 (T1 and T2, respectively), IgM^{hi}IgD^{lo} and IgM^{hi}IgD^{hi}, follicular (FO) B cells (CD21^{hi}CD23^{hi}), and marginal zone (MZ) B cells (CD21^{hi}CD23^{lo}). (e) Individual values for each mouse tested of absolute numbers different B-cell populations, in the spleen obtained from B6 mice $n = 16$, littermate CD21 cre mice $n = 10$, littermate Mb1 cre mice $n = 9$, CD21 cre mice $n = 15$, and Mb1 cre mice $n = 9$. Means and S.D. are indicated. (f and g) Peritoneal lavage was also performed on some animals and the cells obtained were stained by anti-CD5 and anti-B220 Abs. Representative histogram obtained after analysis of cells from the peritoneal lavage by flow cytometry, with the different populations indicated: B-2 B cells (B220^{hi}CD5⁻), B-1a B cells (CD5⁺B220^{lo}), and B-1b B cells (CD5⁻B220^{lo}). (g) Individual values for each mouse tested of percentages of different B-cell populations, in spleens obtained from B6 mice $n = 17$, littermate CD21 cre mice $n = 8$, littermate Mb1 cre mice $n = 4$, CD21 cre mice $n = 15$, and Mb1 cre mice $n = 6$. * $P < 0.05$, ** $P < 0.01$, *** $P < 0.001$ (Mann–Whitney U -test). Hi, high; lo, low

in terms of B-cell proliferation in Mb1 cre and CD21 cre mice stimulated by anti-IgM Abs with or without anti-CD40 stimulation (Figures 4a and b) nor in B-cell survival (Figures 4c and d), compared with their respective littermates. These results are in line with previous reports showing that short-term B-cell stimulation by antigen does not require autophagic activity. In contrast, under lipopolysaccharide (LPS) stimulation, both Mb1 cre and CD21 cre mice showed a significantly reduced survival. LPS is known to drive differentiation of mouse B cells into plasmablasts. These findings highlight a preferential role of autophagy in Ab-secreting cell survival rather than in initial B-cell activation. Incidentally, no exclusive annexin-V staining in CD138-

negative population was found in these conditions, suggesting that B cells upregulate this plasma cell marker normally, but then fail to survive in the absence of autophagy (Figure 5a). Pengo *et al.*¹¹ previously described a defect in ER homeostasis, during plasma cell differentiation in the absence of autophagy. Here, we show further that both CD21 cre and Mb1 cre B cells exhibit an increased mitochondrial content after LPS stimulation as shown by mitotracker staining compared with littermates (Figures 5b and c). Furthermore, mitotracker deep red staining experiments revealed the presence in both deficient models of an increased cell population containing damaged mitochondrial content. We thus propose that autophagy participates in early

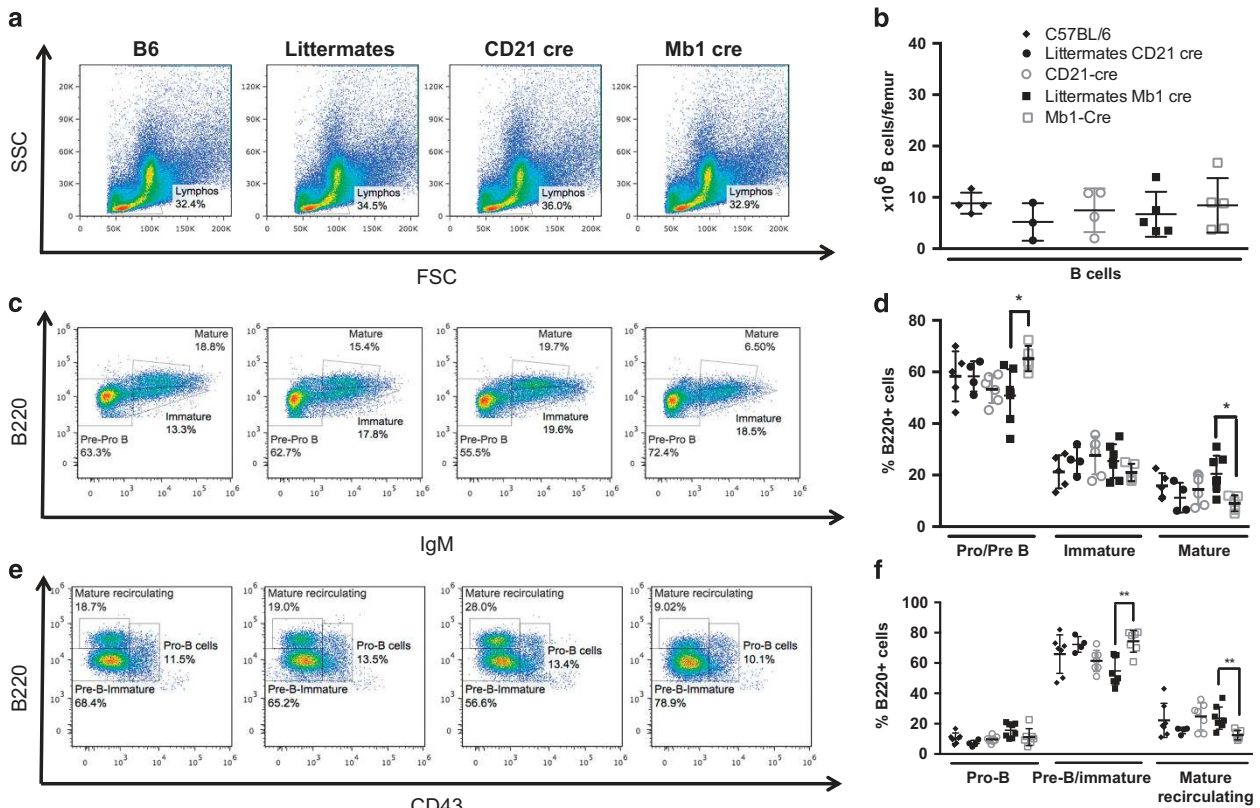


Figure 3 Autophagy is dispensable for B-cell development. Bone marrow cells from one femur of each wild-type C57BL/6 mice (B6), $Atg5^{fl/+}$ CD21 cre (littermates CD21 cre) or $Atg5^{fl/+}$ Mb1 cre (littermates Mb1 cre), $Atg5^{-/-}$ CD21 cre (CD21 cre) or $Atg5^{-/-}$ Mb1 cre (Mb1 cre) were stained with anti-IgM, anti-B220, and anti-CD43 Abs and analysed by flow cytometry. (a) Representative dot plots of FSC and SSC profiles of bone marrow cells. (b) Individual values for each mouse tested of absolute B220+ cell numbers, in the bone marrow obtained from B6 mice $n=4$, littermate CD21 cre mice $n=3$, littermate Mb1 cre mice $n=5$, CD21 cre mice $n=5$, and Mb1 cre mice $n=5$. Means and standard deviations (S.D.) are indicated. (c) Representative dot plots for the expression of B220 and surface IgM, allowing definition of pre-/pro-B cells ($IgM^{-}B220^{lo}$), immature B cells ($IgM^{+}B220^{lo}$), and mature B cells ($IgM^{+}B220^{hi}$). (d) Individual values for each mouse tested of percentages of different B-cell precursors populations depicted in (c), in bone marrows obtained from B6 mice $n=5$, littermate CD21 cre mice $n=4$, littermate Mb1 cre mice $n=7$, CD21 cre mice $n=4$, and Mb1 cre mice $n=5$. Means and S.D. are indicated. (e) Representative dot plots obtained by flow-cytometry analysis, showing the percentages among B220+ cells of pre-B/immature B cells ($CD43^{-}B220^{lo}$), pro-B cells ($B220^{+}CD43^{+}$), and mature recirculating B cells ($B220^{hi}CD43^{-}$). (f) Individual values for each mouse tested of percentages of different B-cell precursors populations depicted in (e), in bone marrows obtained from B6 mice $n=7$, littermate CD21 cre mice $n=4$, littermate Mb1 cre mice $n=7$, CD21 cre mice $n=7$, and Mb1 cre mice $n=8$. Means and S.D. are indicated. * $P < 0.05$, ** $P < 0.01$ significant after Mann-Whitney U -test

plasmablast survival by limiting the potential damages related to increased and/or damaged mitochondrial content.

We then examined short-term humoral responses against the T cell-dependent model antigen OVA (Figure 6a). No difference was observed in the total levels of IgM and IgG in Mb1 cre and CD21 cre mice compared with controls (Figure 6b). Likewise, the anti-OVA IgG secretion in CD21 cre mice and control mice was similar (Figure 6c). This observation could be explained by the fact that in our immunization conditions, long-lived IgG secreting plasma cell differentiation is normal in the absence of autophagy in B cells, and that survival defects might impact IgG secretion at a longer term. However, a significant drop in anti-OVA IgM secretion was observed in both deficient mice (Figure 6c), which could reflect decreased survival of short-lived plasma cells in the absence of autophagy. Our results do not fully recapitulate the conclusions stated in the work of Cenci's group,¹¹ where both IgM and IgG secretions were altered in the absence of autophagy. This could be explained by the difference in the immunization protocol. We thus applied a

protocol closer to the one used by Pengo and immunized Mb1 cre mice and their littermates only once, without boost. Although a slight decrease in both IgG and IgM levels was observed, the differences did not reach significance (Supplementary Figure S2). We cannot totally exclude that other factors linked to immunization, such as the adjuvant for example, may have influenced the data. The use of Freund's adjuvant for repetitively immunizing mice might effectively amplify the deleterious effect of autophagy deletion in short-lived plasmablasts. However, the results we generated in our experimental settings strongly suggest that although antigen-specific responses are altered, continuous differentiation of naïve B cells into plasma cells allows uninterrupted secretion of Ig, as shown by normal levels of total Ig.

Overall, these results demonstrate that in the absence of autophagy in B cells, activation driven by BCR stimulation is largely normal. However, early specific humoral response is compromised, probably due to a defect of short-lived plasma cells, as illustrated by the high mortality rates after stimulating B cells deficient for autophagy by LPS.

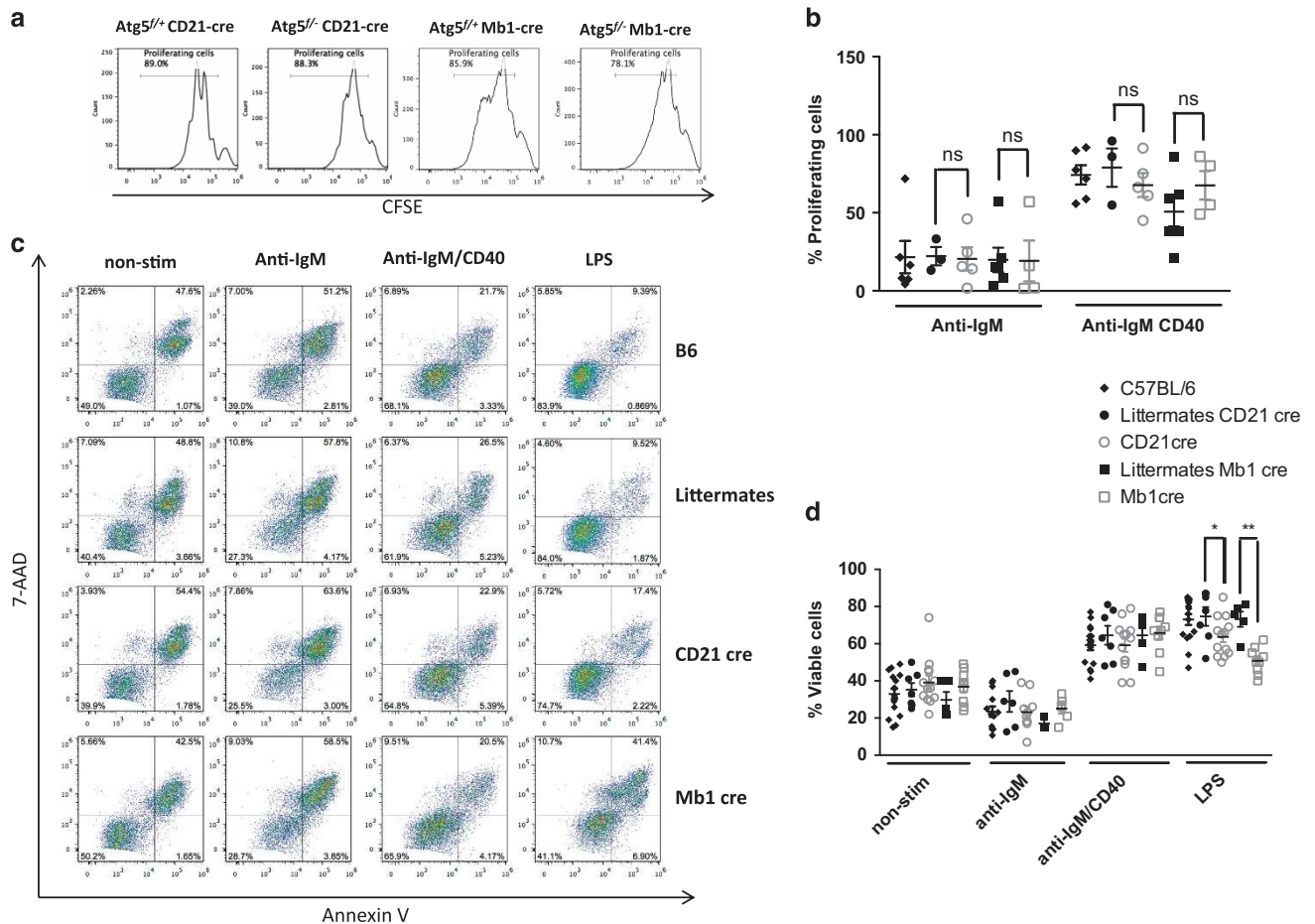


Figure 4 Autophagy is dispensable for B-cell proliferation and survival upon BCR stimulation. Purified splenic B cells from wild-type C57BL/6 mice (B6), Atg5^{+/+} CD21cre (littermates CD21 cre) or Atg5^{-/-} Mb1cre (littermates Mb1 cre), Atg5^{-/-} CD21 cre (CD21 cre), or Atg5^{-/-} Mb1 cre (Mb1 cre) were cultured without any stimulation (non-stim) or with 5 μ g/ml anti-IgM in combination or not with 5 μ g/ml anti-CD40 Abs or with LPS (5 μ g/ml). (a) Cells from the indicated mice were stained with CFSE before culture, and proliferation was assessed by measuring the dilution of the fluorescent signal by flow cytometry after 3 days of culture. Percentages of proliferating cells are indicated in the histograms, for one representative anti-IgM/CD40 stimulation experiment, for each CD21 cre and Mb1 cre mice with their controls. (b) Mean and standard deviation (S.D.) values of the percentages of proliferating cells obtained in four independent experiments. (c) Alternatively, cells were stimulated as described and cell death was assessed by double annexin-V/7-AAD staining allowing to distinguish viable cells (annexin-V⁻7-AAD⁻) early apoptotic cells (annexin-V⁺7-AAD⁻) and late apoptotic/necrotic cells (annexin-V⁺7-AAD⁺). (d) The mean and S.D. values of viable cell proportions obtained in six independent experiments are indicated. ns, non-significant; * $P < 0.05$, ** $P < 0.01$ (Mann-Whitney U -test)

Autophagy in B cells is integral to the long-term maintenance of autoimmune responses. Both macroautophagy and CMA have recently been shown to be deregulated in B cells from lupus-prone mice and patients with lupus.^{19,20} To complete our analysis, we thus asked the question about whether deficiency in *Atg5* could influence autoimmune responses. Owing to the defect in peripheral B-cell homeostasis observed in Mb1 cre mice, these experiments were performed using CD21 cre mice exhibiting a milder phenotype, to be crossed with B6^{*lpr/lpr*} mice. The B6^{*lpr/lpr*} strain develops a mild autoimmunity characterized by the secretion of autoAbs directed against nuclear antigens and Ig and complement deposition in kidneys.²³ Crossed mice were born at the expected Mendelian ratio and did not exhibit differential mortality rates before the age of observation. Compared with CD21 cre Atg5^{+/+} *lpr/lpr* littermate mice (littermates^{*lpr/lpr*}), there was no significant difference in CD21 cre Atg5^{-/-} *lpr/lpr* mice (CD21 cre^{*lpr/lpr*}) when total IgM or specific anti-dsDNA IgM levels were measured (Figure 7a). In sharp contrast, however, CD21 cre^{*lpr/lpr*} mice exhibit a

markedly reduced hypergammaglobulinemia and secreted much less anti-dsDNA IgG (Figure 7a). Several sets of experiments were then designed to investigate whether this reduction could be due to a decreased B-cell survival in peripheral lymphoid organs. No change in splenic B-cell proportions was observed in CD21 cre^{*lpr/lpr*} mice compared with controls (Figure 7b) and no difference was detected in GC area relative to the surface of the spleen section scanned by confocal microscopy (Supplementary Figure S3). These results indicate that in our model of autoimmunity, autophagy does not have any significant role in the early steps of B-cell activation. A slight reduction of splenic plasma cells was noted, but it did not reach statistical significance, consistent with the fact that IgM autoAb levels remain unaffected. These findings may result from a greater replenishment of new short-lived plasma cells in the *lpr* model, compensating their loss in the absence of autophagy.

In contrast to the above observations, a reproducible drop in CD138⁺B220⁻ plasma cell counts was found in the bone marrow of CD21 cre^{*lpr/lpr*} mice, compared with controls

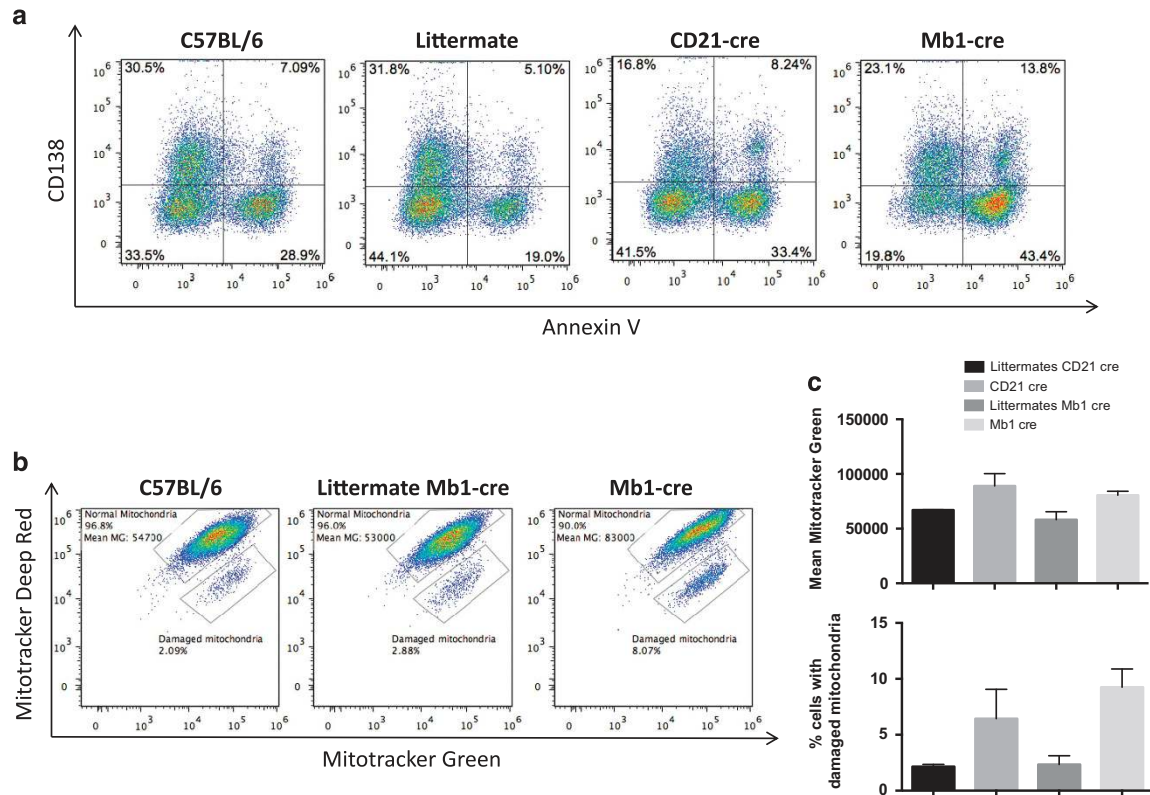


Figure 5 Differentiation of B cells into plasma cells in the absence of ATG5. (a) C57BL/6, *Atg5*^{+/+} CD21 cre (littermate CD21 cre), *Atg5*^{-/-} CD21 cre (CD21 cre), *Atg5*^{+/+} Mb1 cre (littermate Mb1 cre) and *Atg5*^{-/-} Mb1 cre (Mb1 cre) were stimulated by 5 μ g LPS for 48 h. Cells were stained by Annexin-V and anti-CD138 antibody, and analysed by flow cytometry. The percentages indicate the proportion of cells among total events after debris exclusion based on FSC/SSC profile, in the corresponding quadrants. (b and c) The same cells were stained with mitotracker green and deep red. (b) Representative dot plots obtained after analysis of the indicated samples, after gating on live cells based on FSC/SSC profile, showing the repartition of cells that display proportional staining for both markers indicative of normal mitochondrial membrane potential (normal mitochondria). The fluorescence mean of mitotracker green in this population is indicated. The proportion of cells with specific decrease in mitotracker deep red, indicative of a disturbed mitochondrial membrane potential is also indicated (damaged mitochondria). (c) Histograms showing the means of fluorescence in the population 'normal mitochondria' and the means of cell percentage of 'damaged mitochondria' population. The results are obtained on $n=2$ mice for each genotype, the bars stand for S.D.

(Figures 6c and d). For some samples, intracellular IRF4 costaining was performed to ensure that the cell population previously identified corresponds to plasma cells. These results fully agree with the above-described diminished levels of IgG secreted by long-lived CD138⁺B220⁻ plasma cells, which reside in bone marrow niches.

Finally, we investigated the pathophysiological relevance of the decreased autoAb secretion levels observed in CD21cre^{lpr/lpr} mice. In agreement with the above-described results, immunofluorescence imaging of renal glomeruli clearly showed that IgG deposit staining was weaker in CD21cre^{lpr/lpr} mice compared with littermate controls (Figure 8).

Altogether, these results indicate that in a mild spontaneous model of lupus, autophagy is a central component of the long-term maintenance of autoAb production by plasma cells and Ab deposits in target organs, while B-cell proportion remains unaffected.

Discussion

The main purpose of this study was to provide new insight into the role of autophagy in the development of B cells. It was previously assumed that autophagy was important for the

transition from pro- to pre-B cells.⁶ These results were obtained using fetal liver chimaeras with ATG5-deficient cells, in which autophagy was deleted at the early stages of embryonic life, and thus before the initial haematopoietic stem cell development took place. Owing to the major role of autophagy in the survival of haematopoietic stem cells and in lymphocyte precursors,⁸ it thus remained possible that accumulation of defects in the absence of autophagy in B-cell precursors led to the observed defects on pre-B cell survival. Indeed no such defects were observed using CD19, expressed from the pre-B cell stage, to drive cre expression.⁶ It could be argued further that CD19 leads to incomplete ATG5 deletion at this early developmental stage. We thus created a new mouse expressing cre recombinase under the control of the strong Mb1 promoter known to drive very efficient deletion at the pro-B cell stage. In the mice generated in this study, contrary to previous observations, we did not find any developmental blockade at the pro/pre-B cell transition. We thus concluded that autophagy is dispensable for B-cell development in the bone marrow.

However, we found a reproducible decrease in mature recirculating B cells in the bone marrow. These cells

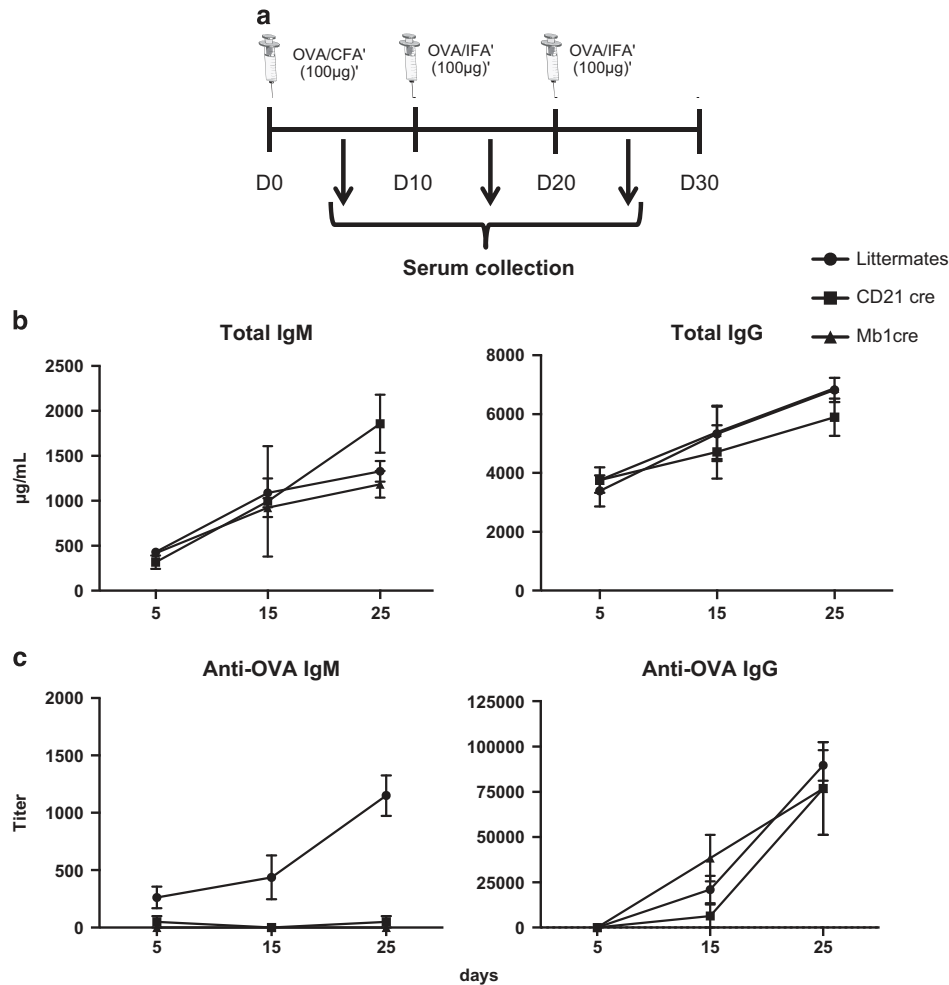


Figure 6 Functional autophagy is important *in vivo* for short-term humoral response. (a) Schematic representation of the immunization protocol used. C57BL/6 mice (B6), *Atg5^{f/+}* CD21 cre or *Atg5^{f/+}* Mb1 cre (littermates), *Atg5^{f/-}* CD21 cre (CD21 cre) or *Atg5^{f/-}* Mb1 cre (Mb1 cre) mice were injected i.p. with OVA in the presence of FA at days 0, 10, and 20. Blood was collected at days 5, 15, and 25. (b) Absolute concentrations (+S.E.M. values) of total IgM and IgG in the serum of immunized animals (littermate mice $n=3$, CD21 cre $n=2$, and Mb1 cre mice $n=2$). (c) Measurement of anti-OVA IgM and IgG Ab titres (+S.E.M. values) in the serum from the immunized animals (littermate mice $n=3$; CD21 cre mice $n=2$; Mb1 cre mice $n=2$)

occupying a specific niche in this central lymphoid organ, are described as long-lived cells, secreting Abs against blood-borne pathogens.²² As CD21 cre mice exhibit no such loss, we cannot totally rule out a developmental issue in B-cell precursors leading to selective defects in this population. It is also possible that the suboptimal deletion of ATG5 in CD21 cre mice is responsible for their normal survival contrary to Mb1 cre mice where the deletion was total. Thus, basal levels of autophagy are particularly necessary for the survival of mature B cells in the bone marrow.

In line with previous reports, we found a strong decrease in B-1a B cells in the peritoneum. Again this loss may be relative to developmental issue, as Mb1 cre mice exhibit this defect but CD21 cre mice did not. Overall, these data support the idea that early precursors of B-1a B cells critically depend on autophagy to generate viable cells at long term.

Interestingly, we also found a diminished survival of B-2 B cells in the peritoneum of both CD21 cre and Mb1 cre mice. This could be explained by the secretory activity of these

cells,^{24,25} or by their nature of mature recirculating cells. In the latter case and in contrast to what occurs in lymphoid organs, a slower replacement rate of dying cells by new B-cell emigrants issued from the bone marrow could account for these observations.

The survival of naive B-2 cells in lymphoid organs was found to be compromised in both CD21 cre and Mb1 cre mice, in a stronger way for the latter deletion strategy. This difference could be linked to the very efficient deletion of ATG5 in Mb1 cre mice, whereas some basal autophagy remained in B cells from CD21 cre mice. It seems that, contrary to what was previously assumed, basal levels of autophagy are indeed required for the survival of B cells in the periphery. This observation may be related to an impairment of homeostatic maintenance, as proliferation and survival upon BCR signaling were normal in both Mb1 cre and CD21 cre mice. Interestingly, in our study, the only effective stimulus leading to survival defect was the one generated by LPS, and this was observed in both our deletion models. LPS is known to drive

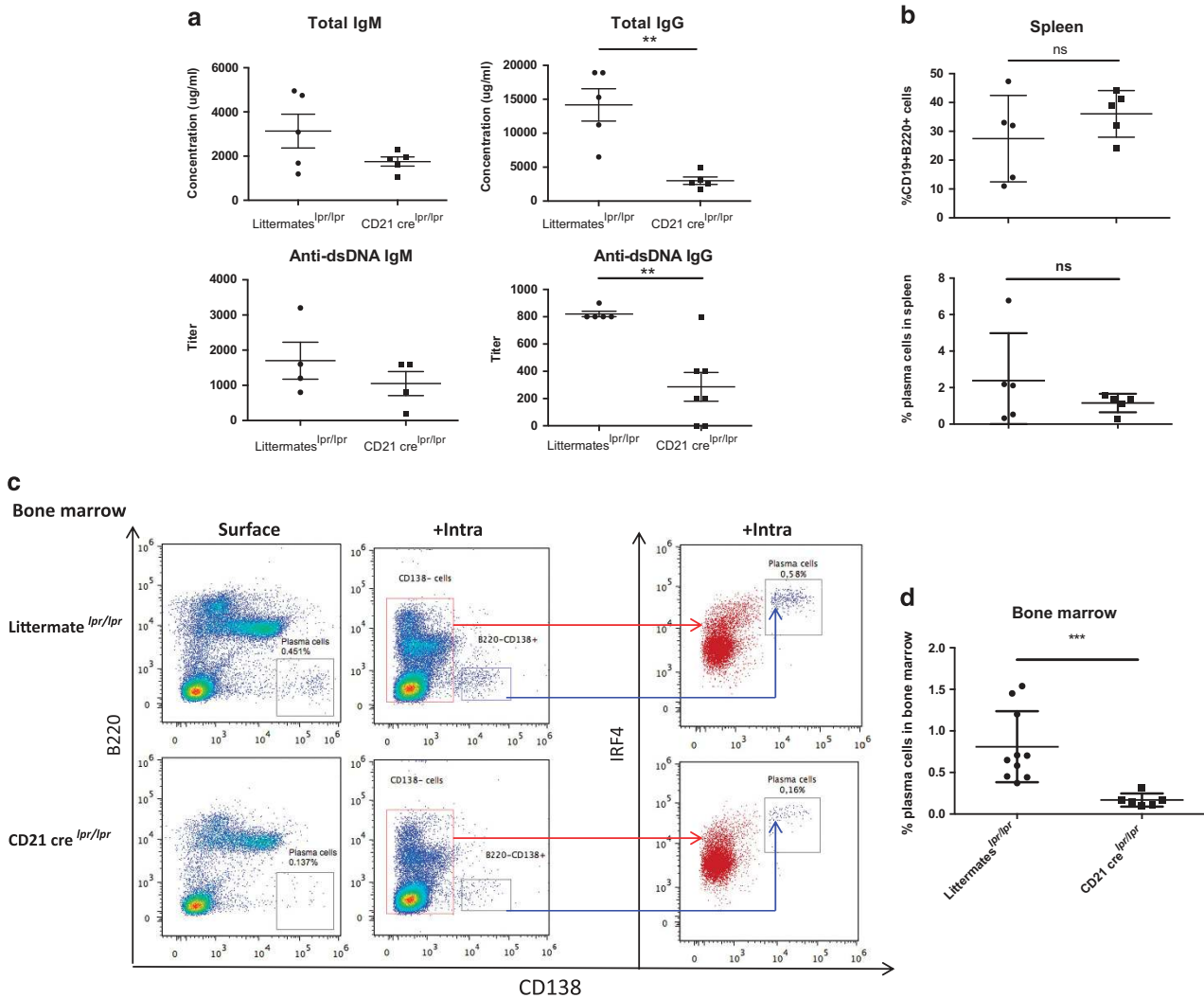


Figure 7 Autophagy is necessary for survival of long-lived plasma cells during autoimmune responses. Mice harbouring the *lpr* mutation on the C57BL/6 background were crossed with *Atg5*^{fl/fl} CD21 cre mice (CD21 cre ^{lpr/lpr}). They were compared with littermate *Atg5*^{fl/fl} CD21 cre mice, also crossed with *lpr* mice (littermates ^{lpr/lpr}), at the age of 9 months. **(a)** Individual values for each mouse assayed for absolute IgG and IgM concentrations in the serum, determined by ELISA and titres of anti-dsDNA IgM and IgG Abs. Means and SEM are represented (at least four mice in each group). **(b)** The spleens of the animals were collected, cells were stained by anti-CD19, anti-CD138, and anti-B220 Abs, and analysed by flow cytometry. Each point represents the value for an individual mouse. The central bar represents the means and the upper and lower bars symbolize the S.D. **(c)** Staining of bone marrow cells collected from one femur per mouse. Each dot plot stands for one representative case for each genotype. On the left, the gate delimiting B220⁺CD138⁺ cells should indicate the percentages of plasma cells resident in the bone marrow (surface). In the middle, results obtained after an intracellular staining of IRF4 molecule performed after surface staining of the previous markers (+intra). The red population corresponding to CD138⁺ cells is IRF4^{low} or IRF4^{int}. The CD138⁺ blue population corresponding to plasma cells is IRF4^{hi}. This latter staining was performed on four littermate ^{lpr/lpr} mice and one CD21 cre ^{lpr/lpr} mouse. **(d)** Percentage of plasma cells among the bone marrow cells for individual mice analysed as in **(c)**. *n* = 10 for littermates ^{lpr/lpr} and *n* = 6 for CD21 cre ^{lpr/lpr}. Mean and S.D. are indicated. ***P* < 0.01, ****P* < 0.001 (Mann-Whitney *U*-test)

the differentiation of mouse B cells into plasmablasts. Thus, the selective survival defect could also be linked to the role autophagy plays in the survival of Ab-secreting cells.

A defective IgM production against the T cell-dependent antigen OVA was observed in both Mb1 cre and CD21 cre mice. In contrast, IgG production against OVA appeared to be normal in the absence of autophagy. A possible explanation for this outcome would be the defective survival of short-lived plasma cells in secondary lymphoid organs in the absence of autophagy while long-lived plasma cells could transiently resist the absence of autophagy. In this setting, defective IgG production could be observed on the long term only. It is also

possible that selection processes allow autophagy-competent cells only to survive, as it has been described in mice with CD19 cre-mediated ATG5 deletion.¹¹ This latter argument remains however uncertain, knowing the very efficient ATG5 deletion observed in our models, especially in Mb1 cre mouse B cells.

To study the long-term impact of autophagy deletion in B cells, we used the spontaneous systemic autoimmunity model driven by the *lpr* mutation on a B6 genetic background.²⁶ This mutation on *Fas* gene leads to secretion of autoAbs directed against nuclear antigens, which can deposit in several organs, especially in the kidneys of affected animals.²³ The pathology

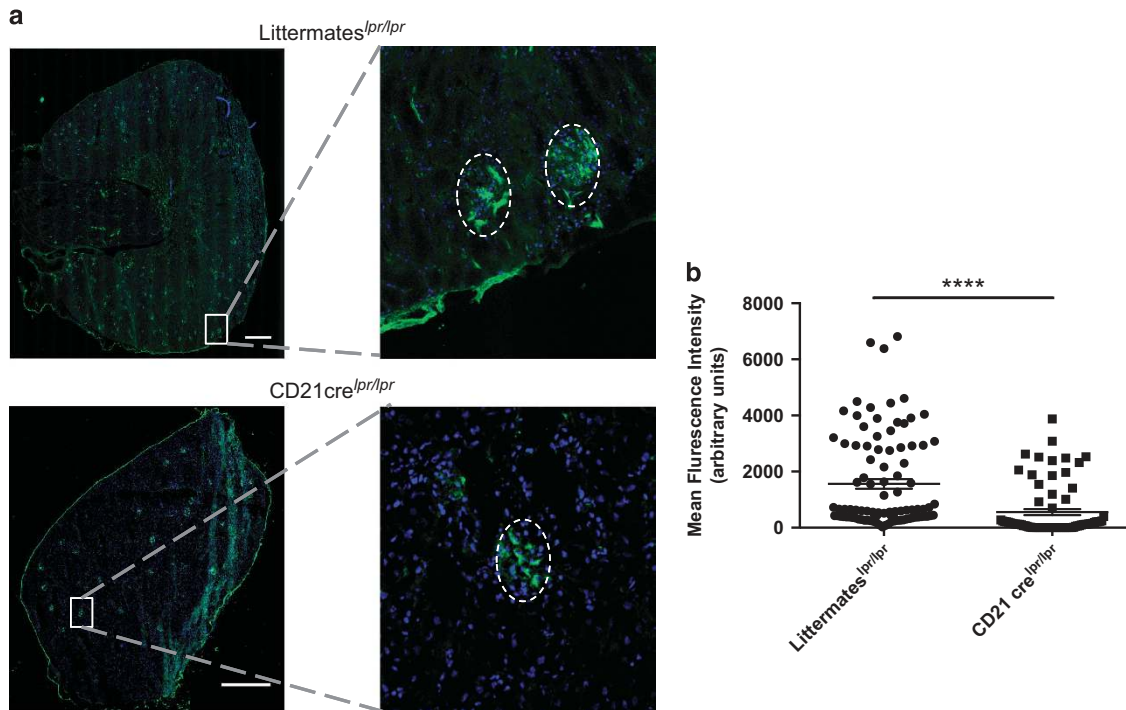


Figure 8 Invalidation of autophagy in B cells reduces IgG deposits in the kidney of lupus-prone mice. Mice bearing the *lpr* mutation on the C57BL/6 background were crossed with $Atg5^{fl/fl}$ CD21 cre mice ($CD21^{cre} lpr/lpr$) and their kidneys were collected at the age of 9 months. $Atg5^{fl/+}$ CD21 cre littermate mice harbouring the *lpr* mutation were used for comparison (littermates lpr/lpr). Organ sections stained with anti-mouse IgG Abs before analysis on a spinning disk confocal microscope. (a) The total section was scanned and a representative image for each genotype is shown on the left. The white bars represent 500 μm . A magnification is indicated on the right to exemplify a glomerulus positive for IgG deposition, delimited by the dotted line. (b) The intensity of IgG staining was determined for each glomerulus as indicated in Materials and methods. Individual values of littermates lpr/lpr $n = 5$ and $CD21^{cre} lpr/lpr$ $n = 4$ ($n = 20$ glomeruli per animal) for each genotype were pooled and plotted on the graph. The bars represent the mean of glomerular IgG staining intensity for each genotype. **** $P < 0.001$ (Mann–Whitney *U*-test)

developed over time, although relatively mild in comparison with MRL/lpr mice, for example, mimicking some lupus features. $Atg5^{fl/fl}$ CD21 cre \times B6 lpr/lpr autophagy-deficient autoimmune mice showed no survival failures in B cells, supporting the minimal role of autophagy in B-cell survival, even in an autoimmune context. In contrast, and in good agreement with data reported in other settings,^{11–13} we found a decrease in plasma cell proportion in the bone marrow reflecting selective defects in long-lived cells. This drop in long-lived Ab-secreting cells may be responsible for the reduction of hypergammaglobulinemia and anti-dsDNA Abs observed in our autophagy-defective mice. Note that we cannot formally exclude a possible contribution of the reduced memory B-cell compartment in *lpr* mice deficient for autophagy.^{12,13} Interestingly, we also found less IgG deposits in the kidneys of $CD21^{cre} lpr/lpr$ mice. Considering the above-described findings, we propose that this feature is mainly due to autophagy impairment in plasma cells, and not in initial B-cell activation, as no major defect in GC formation was noticed.

In summary, using three novel mouse models defective for autophagy process, we report here that autophagy is dispensable for B-2 B-cell development contrary to B-1a B cells and that basal levels of autophagy are required in B cells to maintain their normal number in lymphoid organs. We confirm in a new setting that autophagy is a major player of long-lived B cells and Ab-secreting cell survival. We describe

further that mice exhibiting signs of lupus autoimmunity and in which autophagy was diminished, show significantly less biological (lower anti-dsDNA IgG Ab levels) and clinical (less IgG deposits in their kidneys) lupus features, without having their whole B-cell compartment adversely affected. Therefore, autophagy modulation appears to be a good therapeutic option to limit autoAb-linked inflammation in systemic autoimmunity.

Materials and Methods

Mice. $Atg5^{fl/fl}$ mice, with a flox sequence flanking exon 3 of *Atg5* gene backcrossed on a C57BL/6 (B6) background have been described²⁷ were a kind gift from Prof. N Mizushima. We also used mice with systemic deletion of exon 3 ($Atg5^{+/-}$) to generate $Atg5^{-/-}$ mice. $Atg5^{fl/fl}$ mice were crossed with $Atg5^{+/-}$ CD21 cre²⁸ or $Atg5^{+/-}$ Mb1 cre⁹ mice for B-cell lineage-specific deletion. In all experiments, B6 $Atg5^{-/-}$ CD21 cre or B6 $Atg5^{-/-}$ Mb1 cre mice with B-cell specific deletion of *Atg5* were compared with littermates (B6 $Atg5^{fl/fl}$ CD21 cre mice and $Atg5^{fl/+}$ Mb1 cre mice). In some experiments, B6 $Atg5^{-/-}$ CD21 cre mice were crossed with B6 mice bearing the *lpr* mutation affecting *Fas* gene, driving a spontaneous systemic autoimmunity. In this setting, lupus-prone B6 lpr/lpr $Atg5^{-/-}$ CD21 cre (3 females, 1 male) were compared with age-matched B6 lpr/lpr $Atg5^{fl/+}$ littermates (4 females, 1 male). Mice were genotyped for the *Atg5* alleles (WT, with constitutive or induced deletion) with the primers A (exons 3–1), 5'-GAATATGAAGGCACACCCTGAAATG-3'; B (short 2), 5'-GTACTGCATAATGGTTAACTCTTGC-3'; C (check2), 5'-ACAACGTCGAGCACAGCTGCGCAAGG-3'; D (5L2), 5'-CAGGGAATGGTCTCCAC-3' using PCR (94 °C (4 min); 30 cycles of 94 °C (30 s), 60 °C (30 s), 72 °C (1 min); 72 °C (5 min)). The cre transgene expressed under the control of CD21 promoter was detected with primers cre-F 5'-ACGACCAAGTGACAGCAATG-3'; cre-R 5'-CTCGACCAGTTAGTTACCC-3' and for the cre expressed under Mb1 promoter

with primers, cre-F 5'-ACCTCTGATGAAGTCAGGAAGAAC-3'; cre-R 5'-GGAGA TGTCCTTCACTCTGATTCT-3' using PCR (94 °C (4 min); 25 cycles of 94 °C (30 s), 60 °C (30 s), 72 °C (1 min); 72 °C (5 min)). The *lpr* allele was identified by PCR using a sense primer, 5'-AGGTACAAAAGGTCACCC-3', in intron 2 and two antisense primers, 5'-GATACGAAGATCCTTTCCTGTG-3' and 5'-CAAACGCA GTCAAATCTG CTC-3' using PCR (94 °C (4 min); 30 cycles of 94 °C (45 s), 55 °C (1 min), 72 °C (1 min); 72 °C (5 min)). We genotyped mice with the REDExtract-N-Amp Tissue PCR Kit (Sigma-Aldrich, St. Louis, MO, USA). All mice were bred and maintained in accordance with guidelines of the local Institutional Animal Care and Use Committee (CREMEAS).

Flow cytometry. The majority of antibodies (Abs) used for flow-cytometry analyses were purchased from BD Biosciences (Le Pont-De-Claix, France): allophycocyanin (APC)-Cyanin 7-labelled anti-mouse TCR- β (clone H57-597, 553139), phycoerythrin (PE)-labelled anti-mouse CD69 (clone H1.2F3, 553236), fluorescein isothiocyanate (FITC), APC or peridinin chlorophyll (PerCP) cyanine 5.5-labelled anti-mouse B220 (clone R13-6B2, 553087, 553092, and 552771), FITC-labelled anti-mouse CD3 ϵ (clone 145.2C11, 553061), FITC-labelled anti-mouse CD21/CD35 (clone 7G6, 553818); PE-labelled anti-mouse CD23 (clone B3B4, 553139), APC-labelled anti-mouse CD5 (clone 53-7-3, 550035), APC-labelled anti-mouse CD43 (clone S7, 560663), APC-labelled anti-mouse IgD (clone 11-26 c.2a, 560868), APC-labelled anti-mouse CD19 (clone 1D3, 550992), and APC-labelled anti-mouse CD138 (clone 281-2, 558626). FITC-conjugated polyclonal anti-mouse IgM was purchased from Jackson ImmunoResearch (Newmarket, UK; 115-095-020) and PE-labelled anti-IRF4 from Biologend (San Diego, CA, USA; clone 4.3E4, 646404). Cells were incubated with fluorochrome-conjugated Abs and with unlabelled rat anti-mouse CD16/CD32 monoclonal Ab (mAb, clone 2.4G2, 553142) to block Fc receptors, for 15 min at 4 °C in phosphate-buffered saline (PBS) pH 7.4 containing 2% (v/v) fetal calf serum (FCS). Intracellular staining was performed after surface marker labelling using the FoxP3 detection kit purchased from eBiosciences (San Diego, CA, USA; 00-5523-00). Mitochondria content and membrane potential were measured by incubating cells 30 min at 37 °C in complete medium in the presence of mitotracker green and mitotracker deep red (Fisher Scientific, Pittsburgh, PA, USA; M-7514 and M22426) at the recommended concentrations. Data were collected on a Gallios flow cytometer (Beckman Coulter, Fullerton, CA, USA) and analysed using FlowJo software (FlowJo LLC, Ashland, OR, USA).

Cell culture and isolation. Splenic B cells were collected from B6 *Atg5^{fl/fl}*-CD21 cre, B6 *Atg5^{fl/fl}*-Mb1 cre, B6^{*lpr/lpr*} *Atg5^{fl/fl}*-CD21 cre mice or from littermates and immediately cultured at 37 °C, 5% CO₂ in complete RPMI-1640 medium (Lonza BioWhittaker, Levallois, France) containing 10% FCS, 10 μ g/ml gentamycin (Lonza BioWhittaker), 10 mM HEPES (Lonza, Basel, Switzerland) and 0.05 mM β -mercaptoethanol (Lonza) at a concentration of 5×10^6 cells/ml. Splenic B cells were purified by negative selection. Briefly, spleen cell suspensions were depleted from monocytes, granulocytes, T cells, and NK cells using the Pan B cell isolation Kit II (130-090-862; Miltenyi Biotec, Bergisch-Gladbach, Germany) according to the manufacturer's instructions. Resulting TCR- β /B220⁺ mouse B-cell preparations were >95% pure as determined by flow cytometry. Cells were stimulated with goat F(ab)₂ anti-IgM (Jackson ImmunoResearch; 115-006-020) with or without anti-CD40 Ab (5 μ g/ml, BD Biosciences, clone HM40-3, 553721) or LPS alone (5 μ g/ml, Sigma, Saint-Quentin-en-Yvelines, France). Alternatively, T cells were sorted from spleen cell suspension with the Dynabeads untouched mouse T cell isolation kit (ThermoFisher Scientific, Illkirch, France; 11413D) and were stimulated by anti-CD3 ϵ Ab (clone 145.2C11, 553057) purchased from BD Biosciences. For the analysis of proliferation, cells were stained with 0.5 μ M carboxyfluorescein isothiocyanate succinimidyl ester diacetate (CFSE, Sigma-Aldrich) before the stimulation. Cell death was assessed by Annexin-V-FITC/7-AAD double staining (BD Biosciences, respectively, 559925 and 556419). After acquisition by flow cytometry, proliferation and cell death results were analysed with FlowJo Software.

Immunoblots. The Abs used for western immunoblotting were specific for ACTB (Santa Cruz Biotechnology, Heidelberg, Germany, clone C4, sc-47778), LC3 (MBL, Nagoya, Japan, clone 51-11, ref M115-3), and ATG5 (Polyclonal, Novus, Littleton, CO, USA). In some experiments, lysosomal protease inhibitors E64d and pepstatin A (Sigma-Aldrich; P5318 and E8640) were added at 5 μ g/ml each. When indicated, cells were treated with goat F(ab)₂ anti-IgM (5 μ g/ml, Jackson ImmunoResearch; 115-006-020). To evaluate the autophagosomal membrane load, whole-cell proteins were extracted from cultured cells using Laemmli buffer (125 mM

Tris-HCl, pH 6.8; 2% (w/v) sodium dodecyl sulphate (SDS); 10% (v/v) glycerol; 5% (v/v) β -mercaptoethanol). Cell lysates were separated using 4–20% gradient gels (Bio-Rad, Hercules, CA, USA) and proteins transferred onto a polyvinylidene difluoride membrane. Membranes were blocked with PBS containing 0.1% (v/v) Tween-20 (PBS-T) and 3% (w/v) non-fat dry milk for 1 h and then incubated overnight at 4 °C with 1 μ g/ml anti-LC3 Ab in PBS-T containing 1% non-fat dry milk, or for 1 h at room temperature with 1 μ g/ml anti-ATG5 Ab in PBS-T containing 1% non-fat dry milk. After washing with PBS-T, membranes were incubated for 30 min at room temperature with goat anti-mouse IgG Ab (Southern Biotech, Birmingham, AL, USA; 1030-05) conjugated to horseradish peroxidase (HRP). Signal was detected using enhanced chemiluminescence detection reagents (Immobilion Western, Merck Millipore, Darmstadt, Germany; WBKLS0500). When indicated, LC3-II and ATG5 staining was normalized by densitometry to ACTB staining using the ImageJ Software (National Institute for Health, Washington, DC, USA).

Real-time PCR. Total RNA was isolated from 5×10^6 purified B cells using the RNeasy Mini Kit (Qiagen, Courtabeuf, France, ref 74103) according to the manufacturer's instructions. After treatment by DNase (Qiagen, ref 79254) to remove residual genomic DNA, mRNA was retro-transcribed with the Maxima first-strand synthesis kit for cDNA (ThermoFisher, Illkirch, France). Fifteen nanograms of cDNA was used for real-time PCR (RT-PCR) on StepOne apparatus (ThermoFisher). Briefly, *Atg5* and *Gapdh* cDNA was amplified using Taqman Gene Expression Assays provided by ThermoFisher (ref Mm00504340_m1 and Mm99999915_g1). Amplicons and probe were designed to span two exons, limiting the risk of amplifying residual genomic DNA. Relative *Atg5* mRNA quantifications were made by defining ΔC_T (C_T *Gapdh* - C_T *Atg5* where C_T is 'Cycle Threshold') and $\Delta\Delta C_T$ (ΔC_T sample - ΔC_T of one C57BL/6 mouse sample used for each plate) using StepOne software (ThermoFisher). Results shown represent $2^{-\Delta\Delta C_T}$ values where one same control sample is used on each plate and arbitrarily equal to 1.

Immunization. Eight- to twelve-week-old mice were injected intraperitoneally (i.p.) at days 0, 10, and 20 with the antigen suspension, and bled on days 5, 15, and 25 after the first immunization. Mice received 100 μ g ovalbumin (OVA, Sigma) in complete Freund's adjuvant (CFA, Sigma) for the first injection and 100 μ g OVA in incomplete Freund's adjuvant (IFA, Sigma) for the second and third injections. Alternatively, mice were injected only once with 100 μ g OVA in CFA and were bled at days 7 and 14 to follow the anti-OVA response.

Antibody detection by ELISA. IgG or IgM titres were measured in serum from immunized or lupus-prone mice. To measure anti-OVA specific Abs, 96-well ELISA Maxisorp plates (NUNC, Fisher Scientific) were coated with OVA (10 μ g/ml, Sigma) in 50 mM sodium carbonate buffer (pH 9.6). The wells were blocked with PBS-T 0.1%, 5% (w/v) milk for 1 h at 37 °C and incubated with diluted anti-sera for 1 h at 37 °C. HRP-conjugated anti-mouse isotype-specific Abs (Jackson ImmunoResearch) were used to reveal bound Abs. Absorbance was measured at 450 nm, after revelation with tetramethylbenzidine to the wells, and stop of the reaction by 1M HCl. The same protocol was used for detection of anti-double stranded (ds)DNA Abs except that ELISA plates were coated with 100 ng/ml non-sheared dsDNA (from calf thymus, Sigma-Aldrich) in 25 mM citrate buffer, pH 5. Titres correspond to the inverse of the last dilution giving an absorbance equal to 0.2.

Immunohistofluorescence. Spleen/kidneys were embedded in Tissue-Tek OCT compound (Sakura Finetek, Torrance, CA, USA; 4583) and snap frozen with liquid nitrogen. To visualize IgG deposits in the kidney, tissue sections were then stained with goat anti-mouse IgG-FITC (Southern Biotech; 1030-02) and DAPI. To detect GC in the spleen, tissue sections were stained with peanut agglutinin (PNA, Vector, Burlingame, CA, USA; FL-1071), IgD-APC, and DAPI. Images were acquired with a spinning disk confocal microscope (Zeiss, Oberkochen, Germany) with an A-Plan 20x/0.8 Zeiss $\times 20$ objective. Images were analysed with the ImageJ Software. The quantification of IgG deposits in the kidney was performed as follows: glomeruli were identified via typical structures shaped by DAPI staining. A zone comprising 20 glomeruli was delimited for each kidney section. Fluorescence intensity given by the anti-IgG staining was measured in each glomerulus, and background intensity of the delimited zone was subtracted. The quantification for GC in spleen section was performed by delimiting zones positive for PNA staining, measuring the area of the zone, and by normalizing it to the total area of the scanned section.

Statistical analyses. The data were analysed with the Prism software (GraphPad, San Diego, CA, USA) using two-tailed unpaired *t*-tests or Mann-Whitney *U*-test. Error bars represent standard deviations (SD).

Conflict of Interest

The authors declare no conflict of interest.

Acknowledgements. We thank Prof. Noboru Mizushima for the gift of Atg5^{fl/fl} mice. This work was funded by the French Centre National de la Recherche Scientifique, the Laboratory of Excellence Medalis (ANR-10-LABX-0034) and the EquipEx program I2MC (ANR-11-EQPX-022), Initiative of Excellence (IdEx), Strasbourg University, and the Fondation Arthritis Courtin. JA was a recipient of pre-doctoral fellowship from the Ministère de la Recherche et de l'enseignement supérieur and from Association de Recherche Contre le Cancer; DM was a recipient of pre-doctoral fellowship from the Fond National de Recherche de Luxembourg; FA was a recipient of pre-doctoral fellowship from the Ministère de la Recherche et de l'enseignement supérieur.

Author contributions

JA, JDF and FG performed and designed experiments. DM and FA performed experiments. SM and FG wrote the article.

- Deretic V, Saitoh T, Akira S. Autophagy in infection, inflammation and immunity. *Nat Rev Immunol* 2013; **13**: 722–737.
- Romao S, Gannage M, Munz C. Checking the garbage bin for problems in the house, or how autophagy assists in antigen presentation to the immune system. *Semin Cancer Biol* 2013; **23**: 391–396.
- He MX, McLeod IX, Jia W, He YW. Macroautophagy in T lymphocyte development and function. *Front Immunol* 2012; **3**: 22.
- Paul S, Kashyap AK, Jia W, He YW, Schaefer BC. Selective autophagy of the adaptor protein Bcl10 modulates T cell receptor activation of NF-kappaB. *Immunity* 2012; **36**: 947–958.
- Kovacs JR, Li C, Yang Q, Li G, Garcia IG, Ju S *et al*. Autophagy promotes T-cell survival through degradation of proteins of the cell death machinery. *Cell Death Differ* 2012; **19**: 144–152.
- Miller BC, Zhao Z, Stephenson LM, Cadwell K, Pua HH, Lee HK *et al*. The autophagy gene ATG5 plays an essential role in B lymphocyte development. *Autophagy* 2008; **4**: 309–314.
- Pua HH, Dzhagalov I, Chuck M, Mizushima N, He YW. A critical role for the autophagy gene Atg5 in T cell survival and proliferation. *J Exp Med* 2007; **204**: 25–31.
- Mortensen M, Soilleux EJ, Djordjevic G, Tripp R, Lutteropp M, Sadighi-Akha E *et al*. The autophagy protein Atg7 is essential for hematopoietic stem cell maintenance. *J Exp Med* 2011; **208**: 455–467.
- Hobeika E, Thiemann S, Storch B, Jumaa H, Nielsen PJ, Pelanda R *et al*. Testing gene function early in the B cell lineage in mb1-cre mice. *Proc Natl Acad Sci USA* 2006; **103**: 13789–13794.
- Conway KL, Kuballa P, Khor B, Zhang M, Shi HN, Virgin HW *et al*. ATG5 regulates plasma cell differentiation. *Autophagy* 2013; **9**: 528–537.
- Pengo N, Scolari M, Oliva L, Milan E, Mainoldi F, Raimondi A *et al*. Plasma cells require autophagy for sustainable immunoglobulin production. *Nat Immunol* 2013; **14**: 298–305.
- Chen M, Hong MJ, Sun H, Wang L, Shi X, Gilbert BE *et al*. Essential role for autophagy in the maintenance of immunological memory against influenza infection. *Nat Med* 2014; **20**: 503–510.
- Chen M, Kodali S, Jang A, Kuai L, Wang J. Requirement for autophagy in the long-term persistence but not initial formation of memory B cells. *J Immunol* 2015; **194**: 2607–2615.
- Gros F, Muller S. Pharmacological regulators of autophagy and their link with modulators of lupus disease. *Br J Pharmacol* 2014; **171**: 4337–4359.
- Pierdominici M, Vomero M, Barbati C, Colasanti T, Maselli A, Vacirca D *et al*. Role of autophagy in immunity and autoimmunity, with a special focus on systemic lupus erythematosus. *FASEB J* 2012; **26**: 1400–1412.
- Alessandri C, Barbati C, Vacirca D, Piscopo P, Confaloni A, Sanchez M *et al*. T lymphocytes from patients with systemic lupus erythematosus are resistant to induction of autophagy. *FASEB J* 2012; **26**: 4722–4732.
- Caza TN, Fernandez DR, Talaber G, Oaks Z, Haas M, Madaio MP *et al*. HRES-1/Rab4-mediated depletion of Drp1 impairs mitochondrial homeostasis and represents a target for treatment in SLE. *Ann Rheum Dis* 2014; **73**: 1888–1897.
- Gros F, Arnold J, Page N, Decossas M, Korganow AS, Martin T *et al*. Macroautophagy is deregulated in murine and human lupus T lymphocytes. *Autophagy* 2012; **8**: 1113–1123.
- Clarke AJ, Ellinghaus U, Cortini A, Stranks A, Simon AK, Botto M *et al*. Autophagy is activated in systemic lupus erythematosus and required for plasmablast development. *Ann Rheum Dis* 2015; **74**: 912–920.
- Macri C, Wang F, Tasset I, Schall N, Page N, Briand JP *et al*. Modulation of deregulated chaperone-mediated autophagy by a phosphopeptide. *Autophagy* 2015; **11**: 472–486.
- Hardy RR, Carmack CE, Shinton SA, Kemp JD, Hayakawa K. Resolution and characterization of pro-B and pre-pro-B cell stages in normal mouse bone marrow. *J Exp Med* 1991; **173**: 1213–1225.
- Cariappa A, Mazo IB, Chase C, Shi HN, Liu H, Li Q *et al*. Perinuclear B cells in the bone marrow participate in T-independent responses to blood-borne microbes. *Immunity* 2005; **23**: 397–407.
- Izui S, Kelley VE, Masuda K, Yoshida H, Roths JB, Murphy ED. Induction of various autoantibodies by mutant gene *lpr* in several strains of mice. *J Immunol* 1984; **133**: 227–233.
- Berberich S, Förster R, Pabst O. The peritoneal microenvironment commits B cells to home to body cavities and the small intestine. *Blood* 2015; **109**: 4627–4634.
- Hastings WD, Tumang JR, Behrens TW, Rothstein TL. Peritoneal B-2 cells comprise a distinct B-2 cell population with B-1b-like characteristics. *Eur J Immunol* 2006; **36**: 1114–1123.
- Cohen PL, Eisenberg RA. *lpr* and *gld*: single gene models of systemic autoimmunity and lymphoproliferative disease. *Annu Rev Immunol* 1991; **9**: 243–269.
- Hara T, Nakamura K, Matsui M, Yamamoto A, Nakahara Y, Suzuki-Migishima R *et al*. Suppression of basal autophagy in neural cells causes neurodegenerative disease in mice. *Nature* 2006; **441**: 885–889.
- Kraus M, Pao LI, Reichlin A, Hu Y, Canono B, Cambier JC *et al*. Interference with immunoglobulin (I)galpha immunoreceptor tyrosine-based activation motif (ITAM) phosphorylation modulates or blocks B cell development, depending on the availability of an Igbeta cytoplasmic tail. *J Exp Med* 2001; **194**: 455–469.

Supplementary Information accompanies this paper on Cell Death and Differentiation website (<http://www.nature.com/cdd>)